Article

Insulation Strength and Decomposition Characteristics of a $C_6F_{12}O$ and N_2 Gas Mixture

Xiaoxing Zhang *, Shuangshuang Tian, Song Xiao, Zaitao Deng, Yi Li (iD) **and Ju Tang**

School of Electrical Engineering, Wuhan University, Wuhan 430072, China; tianshuang1002@yahoo.com (S.T.); xiaosongxs@gmail.com (S.X.); 15172313258@163.com (Z.D.); liyi_whuee@163.com (Y.L.); whtangju@whu.edu.cn (J.T.)
* Correspondence: xiaoxing.zhang@whu.edu.cn; Tel.: +86-027-68773771

Abstract: This paper explores the decomposition characteristics of a new type of environmentally friendly insulating gas $C_6F_{12}O$ and N_2 mixed gas under AC voltage. The breakdown behavior of 3% $C_6F_{12}O$ and N_2 mixed gas in quasi-uniform field was investigated through a breakdown experiment. The self-recovery of the mixed gas was analyzed by 100 breakdown experiments. The decomposition products of $C_6F_{12}O$ and N_2 under breakdown voltage were determined by gas chromatography–mass spectrometer (GC-MS). Finally, the decomposition process of the products was calculated by density functional theory, and the ionization energy, affinity, and molecular orbital gap of the decomposition products were also calculated. The properties of the decomposition products were analyzed from the aspects of insulation and environmental protection. The experimental results show that the 3% $C_6F_{12}O$ and N_2 mixed gas did not show a downward trend over 100 breakdown tests under a 0.10 MPa breakdown voltage. The decomposition products after breakdown were CF_4, C_2F_6, C_3F_6, C_3F_8, C_4F_{10}, and C_5F_{12}. The ionization energies of several decomposition products are more than 10 eV. The Global Warming Potential (GWP) values of the main products are lower than SF_6. C_2F_6, C_3F_8, and C_4F_{10} have better insulation properties.

Keywords: $C_6F_{12}O$; N_2; breakdown voltage; decomposition characteristic; density functional theory (DFT)

1. Introduction

Conventional gases (N_2, CO_2, and air) are relatively stable in terms of physical and chemical properties with a low preparation cost. They are widely used as insulating gases in medium- and low-pressure gas insulation equipment such as gas-insulated switchgear (c-GIS) [1]. However, applying reasonable measures to increase the insulation performance of conventional gases, such as increasing the pressure of the gas chamber, increasing the size of the equipment, and using a combination of gas solids, is necessary given their low insulation properties.

Toshiba researchers studied the thermal breaking performance of CO_2 gas by measuring the characteristics of arc current and arc time constant, and they reported the prototype of CO_2 tank circuit breaker with 72 kV rating and breaking capacity of 31.5 kA. However, its volume and weight is approximately 1.5 to 2 times that of the SF_6 circuit breaker at a pressure of 0.7 MPa [2]. Compressed air and N_2 have also been used for 24 kV, 72 kV, and other medium voltage switchgear insulations. To obtain the equivalent of SF_6 gas dielectric strength, the pressure of N_2 must be increased to 3–4 times of SF_6 given that the insulation strength of pure N_2 is low [3]. Korea Hyundai Heavy Industries [4], Toshiba, and other researchers have used air-solid composite insulation technology to enhance the role of its insulation [5]. The results show that the appropriate insulation materials on the high electric field electrode surface coating can effectively improve its electrical strength. Therefore, the current use of

conventional gas in the switch equipment must optimize the structure of the device and increase the pressure and the size of the equipment to increase the production cost of the equipment.

The use of SF_6 gas mixtures are considered given that SF_6 gas in the dielectric strength relative to other insulating medium has evident advantages. The addition of SF_6 can enhance the insulation performance and maintain the pressure to keep the equipment structure compact [6]. However, the "Kyoto Protocol," which was formulated in 1997, emphasized SF_6 as one of the six greenhouse gases with GWP of 23,900 times that of CO_2; moreover, the use of SF_6 should be gradually reduced and an environmentally friendly insulation gas to replace the SF_6 should be selected. Therefore, the recent research and exploration of a new type of environmentally friendly gas has been considered [7]. SF_6 is mainly composed of strong negative gases and mixed gases (CF_3I, $c-C_4F_8$, C_3F_8, and C_2F_6) [8–10]. Among them, the GWP values of $c-C_4F_8$, C_3F_8, and C_2F_6 are less than that of SF_6, but greater than that of CO_2; thus, the greenhouse effect cannot be ignored. CF_3I has acceptable insulation performance and a GWP value of 0. However, the gas in the discharge has a solid iodine precipitation, affecting insulation performance.

$C_6F_{12}O$ is non-combustible and non-toxic and currently limited for use in fire extinguishing agent [11], magnesium treatment, and two-phase immersion cooling system covered gas [12]. $C_6F_{12}O$ molecule is an ozone depletion potential (ODP) gas with a GWP value close to 1 and dielectric strength of approximately 1.7 times that of pure SF_6 gas [13]. The structure of $C_6F_{12}O$ is mainly the combination of the characteristic double and single bonds of ketone carbonyl and its prominent dielectric strength can be attributed to the strong electron absorption capacity of high fluorine content in molecular structure. The mixing ratio in the mixed gas is relatively low (less than 10%) because gas liquefaction temperature is extremely high (liquefaction temperature of 49 °C at 0.1 MPa). The discharge of insulating gas under the insulation defect leads to decomposition, and the insulating properties of the decomposition products are important indexes to evaluate insulating gas. The current decomposition of $C_6F_{12}O$ is limited to the interaction of $C_6F_{12}O$ with oxygen or air in the extinguishing state [14], and the decomposition properties of $C_6F_{12}O$ gas under discharge have not been reported. Therefore, detecting the decomposition products of the insulating gas to ensure its safety, analyzing the physical and chemical properties, and insulating properties of the decomposition products, and evaluating its influence on the gas insulation performance and the environment are necessary.

The present study initially explores the $C_6F_{12}O$ mixed N_2 decomposition characteristics under frequency AC voltage breakdown. Firstly, the decomposition products of $C_6F_{12}O$ and N_2 mixed gas after 0.10 MPa were investigated. Secondly, the change in the surface elements of the electrode was detected using photoelectron spectroscopy. Thirdly, gas decomposition products of the mixed gas are detected by GC-MS. Fourth, binding test results were used to calculate the decomposition process of the products based on density functional theory (DFT), and the ionization energy, affinity, and molecular orbital gap of the decomposition products were calculated. Finally, the properties of the decomposition products and the influence on the insulation properties of the mixed gas were analyzed.

2. Experiment

The experimental wiring diagram of the power frequency voltage experiment platform is shown in Figure 1. The sphere electrodes are placed in the insulating gas chamber, and the electrode material is copper with a diameter of 50 mm and an electrode spacing of 5 mm.

T_1:   Induction voltage regulator with an input voltage of 380 V and an output voltage of 0–400 V;

T_2:   Non-corona test transformer can provide the power frequency test voltage of 100 kV;

R: Protection resistance of R = 10 kΩ, which can protect the transformer from being damaged in breakdown;

C_V: Capacitive divider, in which the test voltage with high amplitude can be converted into the lower value which can be measured directly by the voltmeter;

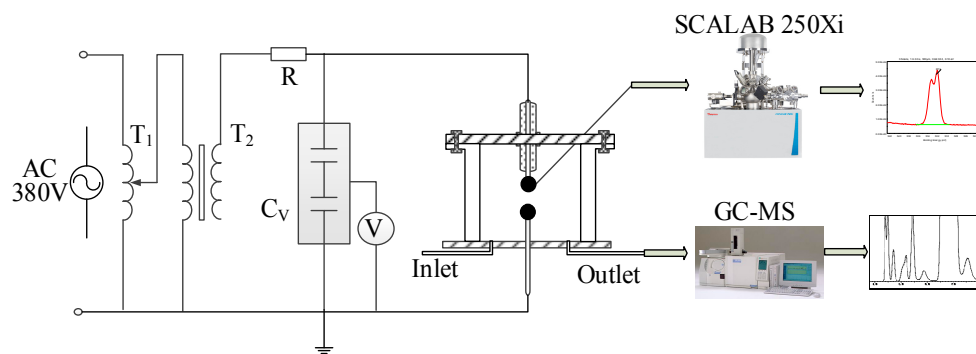V: Voltmeter measures the voltage through the capacitive divider.

Figure 1. Test wiring diagram.

$C_6F_{12}O$ gas is liquid at room temperature because its liquefaction temperature is 49 °C. The saturated vapor pressure of the gas satisfies the Antoine equation, and the saturated vapor pressure of $C_6F_{12}O$ is 40 kPa at 25 °C [13]. The Antoine equation is used to obtain the relation between saturated vapor pressure and the liquefaction temperature of $C_6F_{12}O$:

$$\lg p = -3719.7385/T + 18.180 \tag{1}$$

where T is the liquefaction temperature of gas, and p is the saturated vapor pressure of $C_6F_{12}O$.

According to Dalton's law, ideally, the partial pressure of a gas in the gas mixture is equal to the pressure produced at the same temperature when it occupies the entire container alone, and the total pressure of gas mixture is equal to the sum of the gas partial pressure.

$$P_T = \sum P_i \tag{2}$$

where P_T is the total pressure of gas, and P_i is the partial pressure of each component. The two-component mixed gas is computed as follows:

$$P_T = P_{C6} + P_{N2} = k\,P_T + (1-k)\,P_T \tag{3}$$

where k is the mixing ratio of $C_6F_{12}O$ in the mixed gas. The liquefaction temperature of N_2 is −196 °C [15]. The liquefaction temperature of mixed gas only depends on $C_6F_{12}O$ because the liquefaction temperature of $C_6F_{12}O$ is 49 °C, which is much higher than that of N_2. The minimum operating temperature is −15 °C in the cold condition based on the operating temperature of the medium- and low-voltage equipment of −5 °C to 40 °C, and the main unit of the medium voltage equipment such as GIS must be at −25 °C [16]. To ensure that the mixture gas at less than −15 °C at 0.10 MPa is not liquefied, the mixing ratio of $C_6F_{12}O$ should be less than 5%. We selected 3% $C_6F_{12}O$ mixed N_2 to carry out the breakdown experiment, and the liquefaction temperature of mixed gas is −26 °C.

The breakdown voltage is measured under quasi uniform electric field at 0.10 MPa. The measured breakdown voltage is given as the root mean square (RMS) value. The experimental results show that the breakdown voltage of the 3% $C_6F_{12}O$ mixed N_2 is approximately 1.9 times that of pure N_2 (the breakdown voltage of pure N_2 is approximately 7.6 kV). Thus, a small amount of $C_6F_{12}O$ greatly improves the breakdown performance of N_2. The breakdown voltage has a certain discreteness given the 100 times breakdowns of 3% $C_6F_{12}O/N_2$ gas mixture. However, with the increase in the number of discharge, the breakdown voltage does not decrease, as shown in Figure 2.
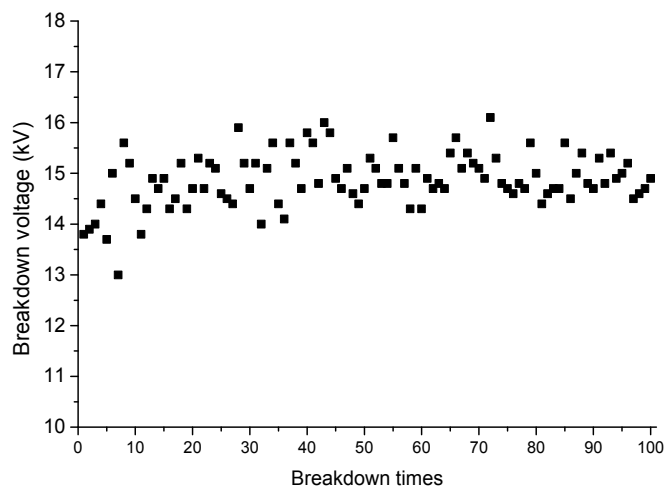
Figure 2. Breakdown voltage of the $C_6F_{12}O/N_2$ mixed gas.

At the end of the experiment, the surface elements of the sphere electrode are tested using Thermo Fisher's ESCALAB 250Xi photoelectron spectroscopy. The gas chromatographic mass spectrometer (GC-MS) equipped with a special capillary column (CP-Sil5CB) is used to separately and qualitatively analyze the decomposition of the characteristic components. A total of 99.999% of the high purity He is used as the GC-MS carrier. The working conditions are as follows: the inlet temperature is 220 °C, the injection volume is 1 mL, the split ratio is 10, the ion source temperature is 200 °C, and the chromatographic mass interface temperature is 220 °C. The mode of ionization is the electron impact ionization (EI).

The sphere electrode surface of the three kinds of elements (C, O, and F) before and after breakdown is scanned using photoelectron spectroscopy. The results are shown in Figure 3. The abscissa is the energy value of the binding energy, whereas the ordinate is the number of photoelectrons per second. After the breakdown, the distribution of the three kinds of elements on the surface of the electrode evidently changed. The C atom increases, and the increase in the F atom is not evident. Before the experiment, the percentage of C, O, and F atoms on the electrode surface is 70.12%, 28.64%, and 1.24%, respectively, and the percentage of atoms on the surface of the electrode after the breakdown is 78.09%, 20.33%, and 1.58%, respectively. The content of C atoms increased by nearly 8%; thus, a small amount of C atoms from the gas are deposited on the surface of the electrode.
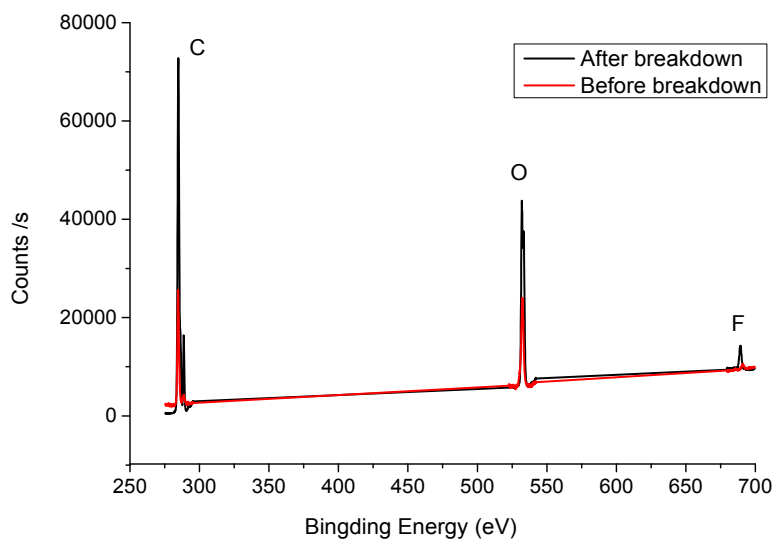

Figure 3. Detection results of the surface elements of the sphere electrode.

The gas in the gas chamber is tested by GC-MS. The detected results of the decomposition products are shown in Figure 4. The purity of $C_6F_{12}O$ gas is 99.5%. The two kinds of chemical impurities are C_2HF_6P and C_6F_{12}, which are detected using a GC-MS spectrum library. The results, before and after the breakdown, are shown in Figure 4. According to standard gas and the corresponding GC-MS spectra similarity detection report (see Figure 5), the main decomposition products of compounds can be produced by the fluorocarbon compounds such as CF_4, C_2F_6, C_3F_8, C_3F_6, C_4F_{10}, and C_5F_{12}. The characteristic peaks of C_3F_6 and C_4F_{10} overlap. The acquisition time of GC-MS is set to 4 min, and the retention time of N_2 is approximately 3 min; thus, N_2 does not form part of the results in Figure 4. The breakdown voltage of the $C_6F_{12}O$ gas decomposition product is mainly fluorocarbon. Although the gas contains N_2, compounds containing N atoms are undetected. The molecular structure of $C_6F_{12}O$ indicates that the formation of the products is mainly due to the formation of free radicals by the breaking of C–C bonds, and the free radicals are bonded to form the corresponding compounds.
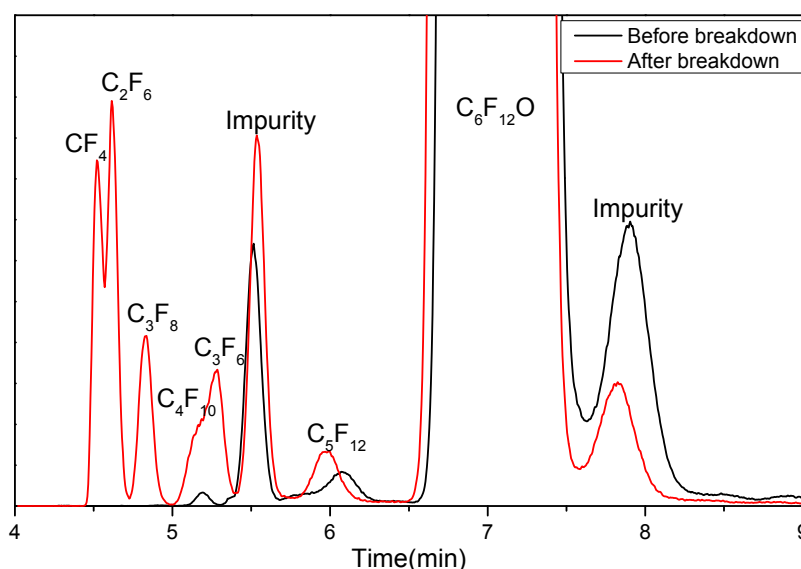

Figure 4. Test results of $C_6F_{12}O/N_2$ mixed gas decomposition components.

3. Decomposition Process Calculation

The experimental detection of the $C_6F_{12}O$ reaction with N_2 shows that the main products are CF_4, C_2F_6, C_3F_8, C_3F_6, C_4F_{10}, and C_5F_{12}, and these products also have certain insulation performance. The decomposition process is calculated using density functional theory (DFT), and the insulating property of several kinds of decomposition products is analyzed by calculating the ionization energy of the molecules, affinity energies, and molecular orbital gaps. The calculation is carried out by Dmol3 in the material studio (MS) computing software. The calculation method of the generalized gradient approximation (GGA) is selected and is based on the optimization of the local density approximation (LDA) functional; thus, GGA has higher accuracy than LDA. The GGA method and the Perdew, Burke, and Enzerhof (PBE) function are used to deal with the electron exchange interaction [17]. The function fitting d and p orbital polarization are used in the atomic orbital calculations through the p polarization dual numerical basis set (Double Numerical Set Plus Polarization Functions, DNP). The energy convergence precision, atomic migration, and energy gradient are set to 1.0×10^{-5} , 0.005, and 0.002 Ha, respectively, and the convergence precision of charge density is 1.0×10^{-6} Ha [18]. The Direct Inversion of Iterative Subspace (DIIS), which is used to improve the convergence rate of self-consistent field charge density, can be used to improve efficiency.

3.1. Formation of Decomposition Products

First, the molecular structure of $C_6F_{12}O$ and several decomposition products are optimized to obtain the lowest stable state of molecular energy. To conveniently express the bond lengths and angles of each molecule, the structure of each molecule and the labeling of C atoms are presented in Figure 5. The optimized bond lengths and angles are shown in Table 1. The results of the references are listed in the table. By contrast, the results of C_3F_8, C_3F_6, C_2F_6, and CF_4 are compared with the references, and the validity and accuracy of the model are verified.
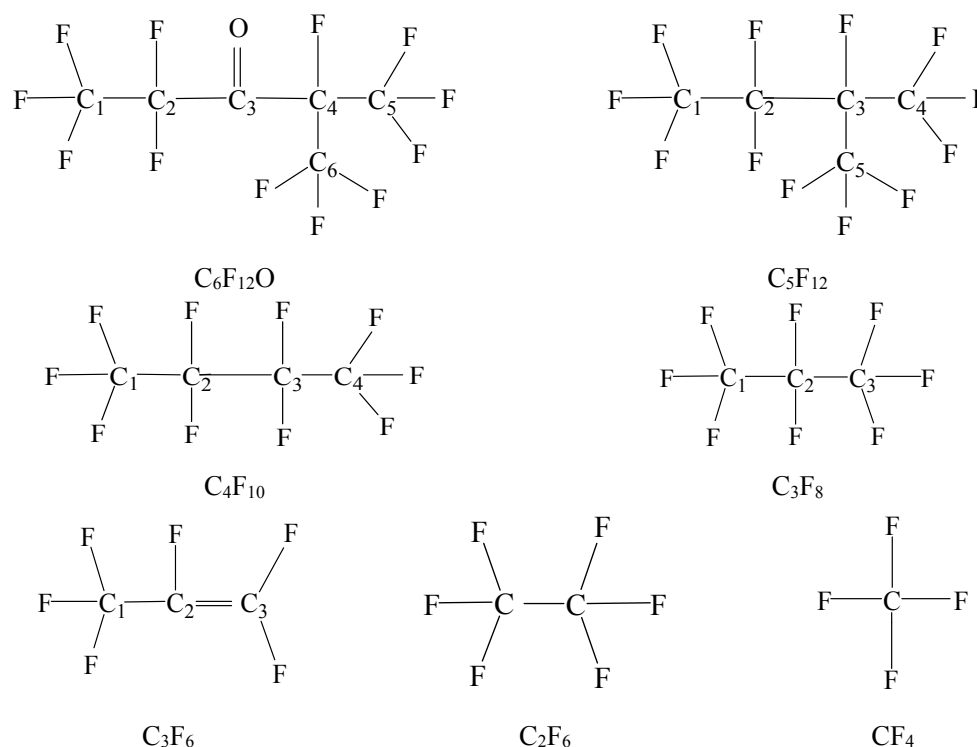
$C_6F_{12}O$

C_5F_{12}

C_4F_{10}

C_3F_8

C_3F_6

C_2F_6

CF_4

Figure 5. Molecular structure.

Table 1. Bond lengths and angles.

Gas	Bond Length			Bond Angle		
Species	Type	Value(Å)	Reference	Type	Value (°)	Reference
$C_6F_{12}O$	F–C$_1$	1.402	-	F–C$_1$–F	108.511	-
	C$_1$–C$_2$	1.566	-	F–C$_2$–F	108.021	-
	F–C$_2$	1.409	-	C$_1$–C$_2$–C$_3$	115.584	-
	C$_2$–C$_3$	1.566	-	C$_2$–C$_3$=O	117.907	-
	C$_3$=O	1.277	-	C$_2$–C$_3$–C$_4$	124.115	-
	C$_3$–C$_4$	1.594	-	C$_3$–C$_4$–C$_5$	113.574	-
	C$_4$–F	1.439	-	F–C$_4$–C$_6$	104.340	-
	C$_4$–C$_5$, C$_4$–C$_6$	1.565	-	F–C$_5$–F	108.519	-
	C$_5$–F, C$_6$–F	1.401	-			-
C_5F_{12}	F–C$_1$	1.348	-	F–C$_1$–F	108.719	-
	C1–C$_2$	1.571	-	F–C$_1$–C$_2$	110.792	-
	C$_2$–C$_3$	1.579	-	F–C$_2$–F	109.044	-
	F–C$_2$	1.361	-	F–C$_2$–C$_3$	107.132	-
	F–C$_3$	1.376	-	F–C$_3$–C$_4$	106.775	-
	C$_3$–C$_4$, C$_3$–C$_5$	1.583	-	C$_1$–C$_2$–C$_3$	118.835	-
	C$_4$–F, C$_5$–F	1.348	-	C$_2$–C$_3$–C$_4$	114.570	-
			-	C$_4$–C$_3$–C$_5$	110.239	-
			-	F–C$_4$–F	107.675	-

Table 1. *Cont.*

Gas	Bond Length			Bond Angle		
Species	Type	Value(Å)	Reference	Type	Value (°)	Reference
C_4F_{10}	$F–C_1$, $F–C_4$ $F–C_2$, $F–C_3$ $C_1–C_2$, $C_3–C_4$ $C_2–C_3$	1.349 1.360 1.568 1.564	-	$F–C_1–F$ $F–C_2–F$, $C_1–C_2–C_3$ $C_2–C_3–C_4$ $C_1–C_2–F$	108.692 109.103 115.210 115.185 107.392	-
C_3F_8	$C_1–C_2$, $C_2–C_3$ $F–C_1$, $F–C_3$ $F–C_2$	1.563 1.348 1.359	1.54 [19] 1.33 [19] 1.34 [19]	$F–C_1–C_2$ $F–C_2–F$ $F–C_2–C_3$ $F–C_3–C_4$ $C_1–C_2–C_3$	108.783 108.892 109.292 107.964 115.580	109.1 [19] 108.6 [19] 109.5 [19] 108.0 [19] 115.2 [19]
C_3F_6	$C_1–C_2$ $C_2=C_3$ $F–C_1$ $F–C_2$ $F–C_3$	1.497 1.341 1.362 1.350 1.324	1.498 [20] 1.329 [20] 1.341 [20] 1.337 [20] 1.329 [20]	$C_2–C_3–C_4$ $C_4–C_3–C_5$ $F–C_4–F$ $F–C_2=C_3$ $F–C_3–F$	108.200 110.645 113.505 118.849 112.210	108.40 [20] - - - 112.04 [20]
C_2F_6	$C–C$ $C–F$	1.591 1.347	1.56 ± 0.03 [21] 1.32 ± 0.01 [21]	$F–C–F$ $F–C–C$	108.648 110.282	- 109.5 ± 1.5 [21]
CF_4	$C–F$	1.341	1.3166 [22] 1.330 ± 0.005 [23]	$F–C–F$	109.471	-

The structure of the C_6F O is shown in Figure 6, and (1)–(4) indicates the position of bond breaking of C–C bond in the molecule.
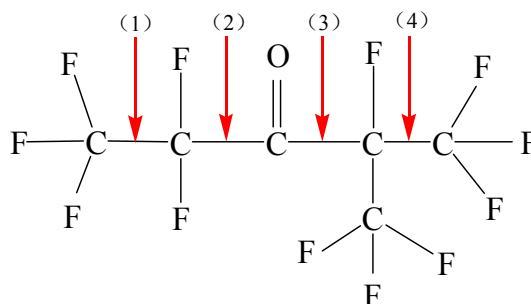
Figure 6. Schematic of the $C_6F_{12}O$ bond breaking.

Calculated by DFT, the four broken bond process and energy changes are as follows:

(1)　$C_6F_{12}O \rightarrow CF_3\bullet + C_5F_9O\bullet$　$\Delta H = 86.7857$ kcal/mol

(2)　$C_6F_{12}O \rightarrow C_2F_5\bullet + C_4F_7O\bullet$　$\Delta H = 85.6439$ kcal/mol

(3)　$C_6F_{12}O \rightarrow C_3F_5O\bullet + C_3F_7\bullet$　$\Delta H = 83.4267$ kcal/mol

(4)　$C_6F_{12}O \rightarrow C_5F_9O\bullet + CF_3\bullet$　$\Delta H = 81.0649$ kcal/mol

By calculating the energy of four C–C bonds, the absorbed energy in the four processes is found to be similar, that is, when the external energy is sufficiently large, the probability of the existence of several free radicals is similar. The free radicals, such as $CF_3\bullet$, $C_2F_5\bullet$ and $C_3F_7\bullet$, can produce F atoms by bond breaking reaction and form relatively stable fluorocarbon compounds, such as CF_4, C_2F_6, C_3F_8, C_3F_6, C_4F_{10}, and C_5F_{12}, between the radical combination process, as shown in Figure 7. $CF_3\bullet$ can be derived from the $C_1–C_2$ breaking and the $C_4–C_5$ or the $C_4–C_6$ breaking (shown in Figure 5).
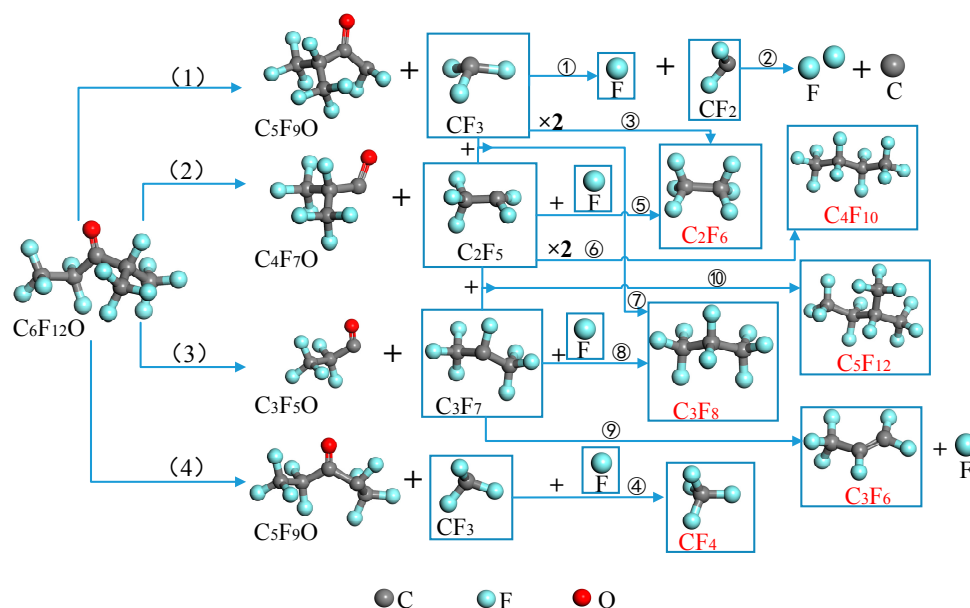
Figure 7. Schematic of the decomposition process.

CF_3 can continue to form CF_2 by breaking C–F, and the calculation in this paper is consistent with the literature [19] (the result in the literature is 84.92 kcal/mol). CF_2 can continue to eliminate F and eventually form a C atom; thus, a significant increase in C elements on the surface of the electrode is observed. The process must absorb the energy of 234.768 kcal/mol.

The numbers ①–⑩ in Figure 7 indicate the reactions and the related reactions is shown in Table 2. C_2F_6 can be formed in two means, and the bond of the two free radicals, CF_3 or C_2F_5 and F, can also be formed. The formation of C_2F_6 has two paths, as shown in the reaction ③ and ⑤. The formation of C_3F_8 also has two paths, as shown in the reaction ⑦ and ⑧ in Figure 7. The formation of C_3F_6 requires $C_3F_7\bullet$ to eliminate F, and requires the C–C single bond to form the C=C double bond. Table 2 presents the main forming process of fluorocarbon, and the barrier energy changes, and the generation process. The energy calculation includes the zero-point vibrational energy (ZPVE) correction value and enthalpy correction.

Table 2. Energy and barrier of decomposition product.

No.	Reaction	Energy of Reactants (Ha)	Energy of Products (Ha)	Temperature Correction Value (298 K) (kcal/mol)	Energy (kcal/mol)	Barrier (kcal/mol)
①	$CF_3\bullet \rightarrow F\bullet + CF_2$:	−337.4509077	−337.3130314	−3.109	83.409	-
②	CF_2: $\rightarrow 2F\bullet + C$	−237.5749908	−237.2185790	11.116	234.768	-
③	$CF_3\bullet + CF_3\bullet \rightarrow C_2F_6$	−674.777429	−674.9387560	−0.238	−101.472	-
④	$CF_3\bullet + F\bullet \rightarrow CF_4$	−437.0751517	−437.2801428	6.345	−122.289	-
⑤	$C_2F_5\bullet + F\bullet \rightarrow C_2F_6$	−674.7368246	−674.9387560	6.444	−120.270	-
⑥	$C_2F_5\bullet + C_2F_5\bullet \rightarrow C_4F_{10}$	−1150.1183793	−1150.2726764	3.302	−93.521	-
⑦	$C_2F_5\bullet + CF_3\bullet \rightarrow C_3F_8$	−912.4463898	−912.6071230	8.819	−92.043	-
⑧	$C_3F_7\bullet + F\bullet \rightarrow C_3F_8$	−912.4310489	−912.6071230	6.755	−103.733	-
⑨	$C_3F_7\bullet \rightarrow C_3F_6 + F\bullet$	−812.7456917	−812.6434617	−3.015	61.135	54.296
⑩	$C_2F_5\bullet + C_3F_7\bullet \rightarrow C_5F_{12}$	−1387.8040065	−1387.9376407	3.565	−80.292	-

Table 2 shows the C–C and C–F bond breaking of $C_6F_{12}O$ to form the free radicals CF_3, C_2F_5, and C_3F_7, and the F atoms, whereas the free combination reaction to form stable fluorocarbon. In addition to the production process of C_3F_6, the other decomposition products generated include an exothermic reaction. The change in energy is the difference between the energy of the reactants. The calculation is carried out in 0 K; thus, the temperature correction is introduced at a normal temperature (298 K). The

formation process of C_3F_6 not only includes the breaking of chemical bonds, but also the formation of chemical bonds. With the transition state search (TS search) activation energy calculation of the process, the energy of 61.135 kcal/mol must be absorbed to generate C_3F_6, and the reaction requires endothermic 54.296 kcal/mol to break the C–F bonds in C_3F_7. The formation processes of CF_4, C_2F_6, C_3F_8, C_4F_{10}, and C_5F_{12} include simple bonding processes, compared with C_3F_6.

3.2. Basic Properties of $C_6F_{12}O$ and Decomposition Products

To analyze the basic properties of $C_6F_{12}O$ and the decomposition products of the molecule, DFT is used to calculate the adiabatic ionization energy of molecules E_{ion}, the adiabatic affinity energy E_{aff}, and the electron orbit distribution. The ionization and affinity energies are calculated by the following:

$$E_{ion} = E_{x+} - E_x \qquad (4)$$

$$E_{aff} = E_x - E_{x-} \qquad (5)$$

where X is a molecule, and X- is a negative ion. X+ is a positive ion. E_{ion} represents the energy required for the loss of electrons and the ability of the gas molecule to bind electrons. E_{aff} is the energy released by the molecules adsorbed on the molecule and the ability of the molecule to adsorb electrons.

The highest occupied molecular orbital (HOMO) and the lowest unoccupied molecular orbital (LUMO) are generally referred to as frontier orbitals. The most active electrons in the electron chemical reaction in the frontline are the core of the chemical reaction. The molecular orbital energy gap E_O is used to describe the molecular activity.

$$E_O = E_{LUMO} - E_{HOMO} \qquad (6)$$

where E_{HOMO} is the energy of the highest occupied molecular orbital, and E_{LUMO} is the energy of the lowest unoccupied molecular orbital. E_O indicates that the electrons in the molecule must be involved in the chemical reaction, which is required to overcome the orbital energy, and in the ability to participate in the chemical reaction. More stable molecules can bind electrons to relatively low levels of energy, and electrons are not easily ionized away from the orbital.

Several decomposition products are calculated using this method, and the comparative results are shown in Table 3. The vertical affinity energy of SF_6 is 0.438 eV, which is consistent with the measured value (0.32 ± 0.15 eV) in the literature [24]. Table 3 shows that the ionization energy of the formation is relatively high; thus, the gas molecules have a strong ability to bind and to not easily lose electrons. The process of adsorption electrons of CF_4, C_2F_6, C_3F_8, C_4F_{10}, and C_5F_{12} need absorb energy, whereas the adsorption electrons of C_3F_6 need release energy, and these energy values are relatively small. From the view of a molecular orbital gap, the difference between various molecules is large. The comprehensive evaluation reveals that the decomposition products after the breakdown of $C_6F_{12}O$ with larger ionization energy have a certain degree of electronic adsorption capacity.

Table 3. Parameter comparison of $C_6F_{12}O$ decomposition products.

Gas	E_{ion} (eV)	E_{aff} (eV)	E_O (eV)	Insulation Strength Relative to SF_6 [25–27]	Boiling Point (°C) [27,28]	GWP (100 Years) [27,29]	Lifetime (Years) [27,30,31]
SF_6	15.153	0.438	8.999	1	−63	23900	3200
$C_6F_{12}O$	11.408	0.817	6.120	2.70	49	~1	5 days
CF_4	15.965	−1.253	12.590	0.39	−186.8	6300	50,000
C_2F_6	14.796	−1.208	11.570	0.78–0.79	−78	9200	10,000
C_3F_8	14.208	−0.673	10.330	0.96–0.97	−37	7000	2600
C_3F_6	11.759	1.755	5.129	-	−28	-	<10
C_4F_{10}	11.674	−1.841	7.973	1.25, 1.31	−2	7000	2600
C_5F_{12}	14.657	−0.906	7.680	-	28	7280	>2000

Table 3 shows that the ionization energy of the products, which is more than 10 eV, is large. The insulation strength of CF_4 gas is approximately 39% of SF_6, and the insulation performance of C_2F_6 is approximately 80% of SF_6. The insulation performance of SF_6 is close to C_3F_8, whereas C_4F_{10} has insulation properties that are even better than SF_6. The liquefaction temperature of the decomposition products is lower than that of $C_6F_{12}O$, and the concentration of the product is much lower than that of $C_6F_{12}O$. The main products are Perfluorinated compounds (PFCs), which impact the environment [29]. However, the GWP of the product is less than that of SF_6. Thus, the product does not damage the environment.

4. Conclusions

The present study explores the decomposition products of $C_6F_{12}O/N_2$ gas mixture at 0.10 MPa under AC breakdown voltage. The decomposition process of $C_6F_{12}O$ is calculated by DFT. The main conclusions are as follows:

The breakdown voltage of 3% $C_6F_{12}O$ and N_2 mixed gas at 0.10 MPa is 1.9 times that of pure N_2. The decomposition products after gas breakdown include CF_4, C_2F_6, C_3F_6, C_3F_8, C_4F_{10}, and C_5F_{12}, and include the surface detection in the sphere electrode of C, O, and F, in which the number of C atoms increases. The experimental results show that the 3% $C_6F_{12}O$ and N_2 mixed gas did not show a downward trend over 100 times breakdown tests under a 0.10 MPa breakdown voltage.

The decomposition process of $C_6F_{12}O$ is calculated, and the C–C and C–F bonds in the $C_6F_{12}O$ molecule break down to form the free radicals CF_3, C_2F_5, and C_3F_7, as well as F atoms, in which the four kinds of C–C bonds have a minimal difference in the energy of breaking bonds.

The decomposition products of $C_6F_{12}O$ have an ionization energy greater than 10 eV. The GWP values of decomposition products are all less than that of SF_6; hence, they have no significant impact on the environment. The products C_2F_6, C_3F_8, and C_4F_{10} can still maintain high insulation performance; thus, the breakdown voltage does not decrease after 100 breakdowns.

References

1. Rokunohe, T.; Yagihashi, Y.; Endo, F.; Oomori, T. Fundamental insulation characteristics of air; N_2, CO_2, N_2/O_2, and SF_6/N_2 mixed gases. *Electr. Eng. Jpn.* **2006**, *155*, 9–17. [CrossRef]
2. Nishiwaki, S.; Koshizuka, T.; Uchii, T.; Kawano, H. Discussions on post arc current of a CO_2 circuit breaker. In Proceedings of the 17th International Conference on Gas Discharges and Their Applications, Cardiff, UK, 7–12 September 2008.
3. Uchiii, A.M.T.; Koshizuka, T.; Kawano, H. Thermal interruption capabilities of CO_2 gas and CO_2-based gas mixtures. In Proceedings of the 18th International Conference on Gas Discharges and Their Applications, Greifswald, Germany, 5–10 September 2010.
4. Lim, D.Y.; Bae, S. Study on oxygen/nitrogen gas mixtures for the surface insulation performance in gas insulated switchgear. *IEEE Trans. Dielectr. Electr. Insul.* **2015**, *22*, 1567–1576. [CrossRef]
5. Kim, J.Y.; Kim, Y.M.; Seok, B.Y.; Kwon, J.H.; Lim, K.J. A study on the lightning impulse breakdown characteristics of dry air for design of eco-friendly electric power apparatus. In Proceedings of the 18th International Symposium on High Voltage Engineering, Seoul, Korea, 25–30 August 2013.
6. Koch, H.; Hopkins, M. Overview of gas insulated lines (GIL). In Proceedings of the Power Engineering Society General Meeting, San Francisco, CA, USA, 12–16 June 2005.
7. Zhang, X.; Xiao, S.; Zhou, J.; Tang, J. Experimental analysis of the feasibility of CF_3I/CO_2 substituting SF_6 as insulation medium using needle-plate electrodes. *IEEE Trans. Dielectr. Electr. Insul.* **2014**, *21*, 1895–1900. [CrossRef]
8. Zhang, X.; Xiao, S.; Han, Y.; Cressault, Y. Experimental studies on power frequency breakdown voltage of CF_3I/N_2 mixed gas under different electric fields. *Appl. Phys. Lett.* **2016**, *108*, 092901-1–092901-4. [CrossRef]

9.　Wu, B.T.; Xiao, D.M.; Liu, Z.S.; Zhang, L.C.; Liu, X.L. Analysis of insulation characteristics of c-C_4F_8 and N_2 gas mixtures by the Monte Carlo method. *J. Phys. D Appl. Phys.* **2006**, *39*, 4204–4207. [CrossRef]

10.　Okabe, S.; Wada, J.; Ueta, G. Dielectric properties of gas mixtures with C_3F_8/C_2F_6 and N_2/CO_2. *IEEE Trans. Dielectr. Electr. Insul.* **2015**, *22*, 2108–2116. [CrossRef]

11.　Linteris, G.T.; Babushok, V.I.; Sunderland, P.B.; Takahashi, F.; Katta, V.R.; Meier, O. Unwanted combustion enhancement by $C_6F_{12}O$ fire suppressant. *Proc. Combust. Inst.* **2013**, *34*, 2683–2690. [CrossRef]

12.　Tuma, P.E. Fluoroketone $C_2F_5C(O)CF(CF_3)_2$, as a Heat Transfer Fluid for Passive and Pumped 2-Phase Applications. In Proceedings of the Annual IEEE Semiconductor Thermal Measurement and Management Symposium, San Jose, CA, USA, 16–20 March 2008.

13.　Mantilla, J.D.; Gariboldi, N.; Grob, S.; Claessens, M. Investigation of the insulation performance of a new gas mixture with extremely low GWP. In Proceedings of the IEEE Electrical Insulation Conference, Philadelphia, PA, USA, 8–11 June 2014.

14.　Xu, W.; Jiang, Y.; Ren, X. Combustion promotion and extinction of premixed counterflow methane/air flames by $C_6F_{12}O$ fire suppressant. *J. Fire Sci.* **2016**, *34*, 289–304. [CrossRef]

15.　Deng, Y.; Li, B.; Xiao, D. Analysis of the insulation characteristics of C_3F_8 gas mixtures with N_2 and CO_2 using Boltzmann equation method. *IEEE Trans. Dielectr. Electr. Insul.* **2015**, *22*, 3253–3259. [CrossRef]

16.　Hyrenbach, M.; Hintzen, T.; Muller, P.; Owens, J. Alternative gas insulation in medium-voltage switchgear. In Proceedings of the 23th international conference on electricity distribution, Lyon, France, 15–18 June 2015.

17.　Perdew, J.P.; Wang, Y. Accurate and simple analyticre presentation of the electron-gas correlation energy. *Phys. Rev. B* **1992**, *45*, 13244–13249. [CrossRef]

18.　Monkhorst, H.; Pack, J. Special points for Brillouin-zone integrations. *Phys. Rev. B* **1976**, *13*, 5188–5192. [CrossRef]

19.　Zhang, X.; Xiao, S.; Zhang, J.; Li, C.; Dai, Q.; Han, Y. Influence of humidity on the decomposition products and insulating characteristics of CF_3I. *IEEE Trans. Dielectr. Electr. Insul.* **2016**, *23*, 819–828. [CrossRef]

20.　Ai, L.L.; Duan, X.M.; Liu, J.Y. Theoretical studies on the reaction mechanism of $CF_3CF=CF_2$ with OH. *Comput. Theor. Chem.* **2013**, *1013*, 15–22. [CrossRef]

21.　Swick, D.A.; Karle, I.L. Structure and Internal Motion of C_2F_6 and Si_2Cl_6 Vapors. *J. Chem. Phys.* **1955**, *23*, 1499–1504. [CrossRef]

22.　Carroll, T.X.; Børve, K.J.; Sæthre, L.J.; Bozek, J.D.; Kukk, E.; Hahne, J.A.; Thomas, T.D. Carbon 1s photoelectron spectroscopy of CF_4 and CO: Search for chemical effects on the carbon 1s hole-state lifetime. *J. Chem. Phys.* **1999**, *116*, 10221–10228. [CrossRef]

23.　Garg, S.K.; Davidson, D.W.; Ripmeester, J.A. Analysis of NMR lineshapes of rigid-lattice multispin systems II. Bond length and chemical shielding in CF_4. *J. Magn. Reson.* **1979**, *36*, 325–331. [CrossRef]

24.　Hubers, M.M.; Los, J. Ion pair formation in alkali-SF_6 collisions: Dependence on collisional and vibrational energy. *Chem. Phys.* **1975**, *10*, 235–259. [CrossRef]

25.　Wada, J.; Ueta, G.; Okabe, S.; Hikita, M. Dielectric properties of gas mixtures with per-fluorocarbon gas and gas with low liquefaction temperature. *IEEE Trans. Dielectr. Electr. Insul.* **2016**, *23*, 838–847. [CrossRef]

26.　Devins, J.C. Replacement Gases for SF6. *IEEE Trans. Dielectr. Electr. Insul.* **1980**, *EI-15*, 81–86. [CrossRef]

27.　Deng, Y.; Xiao, D. Analysis of the insulation characteristics of CF_3I gas mixtures with Ar, Xe, He, N_2, and CO_2 using Boltzmann equation method. *Jpn. J. Appl. Phys.* **2014**, *53*, 096201. [CrossRef]

28.　Takahashi, K.; Itoh, A.; Nakamura, T.; Tachibana, K. Radical kinetics for polymer film deposition in fluorocarbon (C_4F_8, C_3F_6, and C_5F_8) plasmas. *Thin Solid Films* **2000**, *374*, 303–310. [CrossRef]

29.　Ivy, D.J.; Rigby, M.; Baasandorj, M.; Burkholder, J.B.; Prinn, R.G. Global emission estimates and radiative impact of C_4F_{10}, C_5F_{12}, C_6F_{14}, C_7F_{16} and C_8F_{18}. *Atmos. Chem. Phys.* **2012**, *12*, 7635–7645. [CrossRef]

30.　Ravishankara, A.R.; Solomon, S.; Turnipseed, A.A.; Warren, R.F. Atmospheric lifetimes of long-lived halogenated species. *Science* **1993**, *259*, 194–199. [CrossRef] [PubMed]

31.　Surhone, L.M.; Timpledon, M.T.; Marseken, S.F. Novec 1230. *Landolt Börnstein Group IV Phys. Chem.* **2010**, *26*, 263–291.